Structural and Energetic Properties of Ni−Cu Bimetallic Clusters

Elisaveta Hristova, Yi Dong, Valeri G. Grigoryan, and Michael Springborg*

Physical and Theoretical Chemistry, University of Saarland, 66123 Saarbrücken, Germany

Received: February 22, 2008; Revised Manuscript Received: June 9, 2008

The lowest-energy structures for all compositions of Ni_nCu_m bimetallic clusters with $N = n + m$ up to 20 atoms, $N = 23$, and $N = 38$ atoms have been determined using a genetic algorithm for unbiased structure optimization in combination with an embedded-atom method for the calculation of the total energy for a given structure. Comparing bimetallic clusters with homoatomic clusters of the same size, it is shown that the most stable structures for each cluster size are composed entirely of Ni atoms. Among the bimetallic clusters in the size range $N = 2-20$, the $Ni_{N-1}Cu_1$ clusters possess the highest stability. Further, it has been established that most of the bimetallic cluster structures have geometries similar to those of pure Ni clusters. The size $N = 38$ presents a special case, as the bimetallic clusters undergo a dramatic structural change with increasing atom fraction of Cu. Moreover, we have identified an icosahedron, a double, and a triple icosahedron with one, two, and three Ni atoms at the centers, respectively, as particularly stable structures. We show that in all global-minimum structures Ni atoms tend to occupy mainly high-coordination inner sites, and we confirm the segregation of Cu on the surface of Ni−Cu bimetallic clusters predicted in previous studies. Finally, it is observed that, in contrast to the bulk, the ground-state structures of the 15-, 16-, and 17-atom bimetallic clusters do not experience a smooth transition between the structures of the pure copper and the pure nickel clusters as a function of the relative number of the two types of atoms. For these sizes, the concentration effect on energy is more important than the geometric one.

I. Introduction

During the last few decades, clusters have attracted considerable interest both from basic science and for applications. Their partly controllable, unique physical and chemical properties can be related to the large surface-to-volume ratio as well as to finite-size or quantum-confinement effects.[1–3] Thus, for clusters containing one type of atoms, the properties can be varied simply by varying the size of the clusters.

An additional degree of freedom for tuning the materials properties is provided by clusters containing not one but two different types of atoms. Such bimetallic clusters have received considerable attention because of their special chemical and physical properties.[4–7] A change in the concentration under the conditions of quantum-confinement effects may result in new types of structures,[8–11] including, for example, core−shell structures.[12–14] Moreover, these materials possess, for chemical applications, interesting enhanced bifunctional catalytic properties that have made them attractive candidates for various chemical applications.[15,16] Thus, considering, for example, the case of a nickel−copper alloy, the substitution of nickel atoms by copper atoms adds extra electrons to the system. The degree to which the d band is filled can affect the catalytic activity. Thus, by varying the composition of such alloy clusters, it is possible to influence the selectivity of a catalyst and improve the catalytic properties of the heteroatomic clusters as compared to their monometallic counterparts. Furthermore, bimetallic clusters are also interesting candidates for use in nanoelectronics.[17,18]

To optimize the materials properties for a given application, it is of paramount importance to have an accurate understanding of the relation between composition/cluster size on the one side and property on the other. Although experimental studies can provide much of this information, a full characterization of the experimentally studied systems is often lacking, suggesting that additional, theoretical studies can be helpful. However, only through precise information on the structure of the lowest total energy may one be able to calculate the properties of interest. Also, even for clusters with only one type of atom, it is overwhelmingly demanding to identify this structure for clusters with just around 10−20 atoms when no assumption is made on the structure.

A nanoalloy cluster distinguishes drastically from a homoatomic cluster in the number of different structures resulting by the permutation of the unlike atoms. For a one-component cluster, different isomers differ by the geometrical arrangement of the atoms. For a two-component cluster, however, different isomers may be obtained by interchanging atoms of the different types without changing the geometrical arrangement of the atoms. Jellinek and co-workers introduced in 1996 the term "homotops"[19,20] for such structures. The number of homotops (topological isomers) for a A_nB_m cluster, $P_{n,m}$, is given through

$$P_{n,m} = \frac{(n+m)!}{n!\,m!} \tag{1}$$

If we consider all possible replacements of 10 Cu atoms by Ni atoms in an isomer of Cu_{20}, for example, the number of combinations is 184 756. Because of this large number of homotops that in addition may have only small total-energy differences, a global optimization becomes a very demanding task.

Studies of the properties of a larger series of A_nB_m clusters have to rely on simplified descriptions of the interatomic interactions. In this case, an extra complication may show up; that is, it is necessary to consider not only A−A and B−B interactions, but also A−B interactions, and all of those may depend indirectly on the local and global concentrations of the two types of atoms.

* Corresponding author. E-mail: m.springborg@mx.uni-saarland.de.

10.1021/jp801837d CCC: $40.75
Published on Web 08/05/2008

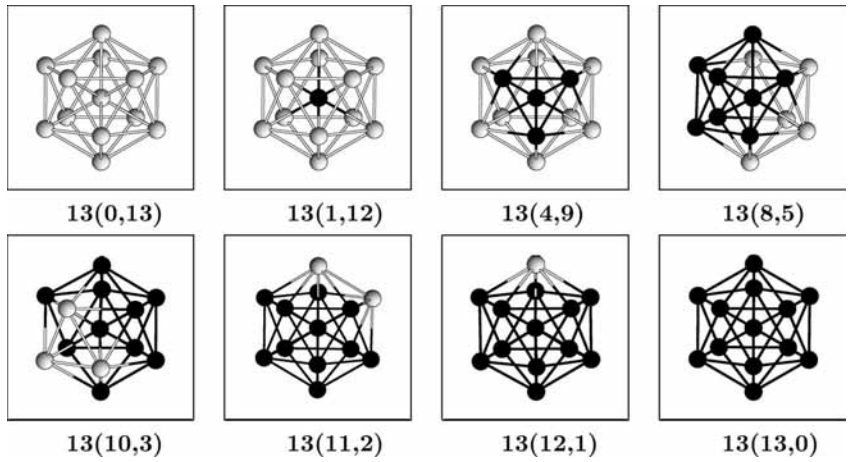

Figure 1. The energetically lowest isomers of Ni_nCu_m clusters for a fixed value of $N = 13$. The dark atoms mark the Ni atoms.

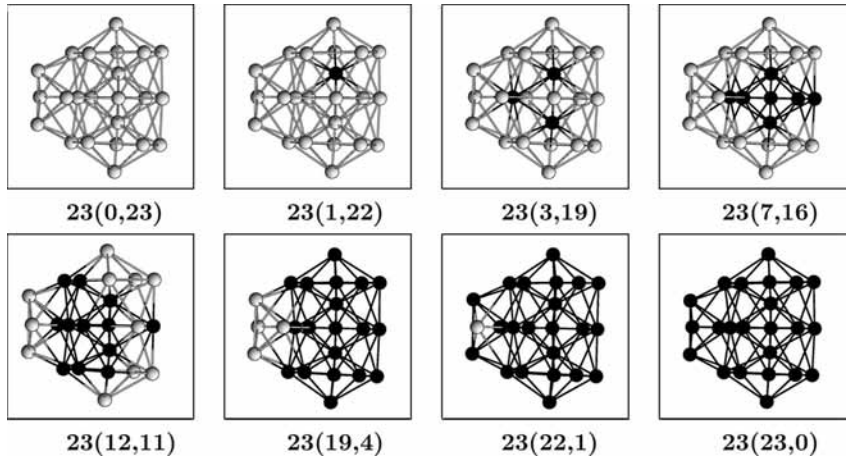

Figure 2. The energetically lowest isomers of Ni_nCu_m clusters for a fixed value of $N = 23$.

Most earlier theoretical studies have assumed that a structure that is particularly stable for the pure A_N and/or B_N clusters, also will be so for the A_nB_m ($n + m = N$). This is, for example, the case for the study of Montejano-Carrizales et al.,[21] who studied the structure and stability of Cu_nNi_m and Cu_nPd_m, $N =$ 55 and 147, and in particular explored whether segregation or mixing would be found. In similar studies, Rey et al.[22] considered Ni_nAl_m with $N = 13$, 19, and 55, and López et al.[23] studied Cu_nAu_m with $N = 13$ and 14, whereby molecular-dynamics simulations were used in identifying the structures of the lowest total energy. Hsu and Lai[24] used a genetic algorithm and the basin-hopping approach in optimizing the structures of Cu_nAu_m, $N = 38$. Cheng et al.[25] used Monte-Carlo simulations in studying the temporal behavior of the structural properties of Cu_nAu_m, $N = 55$. Only in two studies, by Lordeiro et al.[8] and by Bailey et al.,[26] a systematic study of the structural properties of a whole class of bimetallic clusters, Cu_nAu_m with $N \leq 30$ in the first case, and Ni−Al with up to 55 atoms in the second case, has been presented. Finally, the results of a number of studies on the structural and thermodynamic properties (often with special emphasis on segregation and/or the occurrence of core−shell structures) of selected larger bimetallic clusters have been presented, too (see, for example, refs 27–32).

In this study, we will concentrate on the Ni−Cu system. In the past, for a long time this system has been considered to be a classical example for a substitutional solid solution because it seemed to exhibit complete miscibility over the whole range of concentrations. However, experiments[33,34] have shown that bulk Ni−Cu alloys in fact tend to phase separate. The latest phase diagram of the bulk alloy presents a miscibility gap at a critical point of 65.6% Ni and 627.5 K.[36] To the best of our knowledge, experiments on Ni−Cu clusters have not been performed so far. Furthermore, there are only few theoretical studies on Ni−Cu clusters that are neither systematic nor unbiased. Mainardi and Balbuena[37,38] have predicted the surface segregation of Cu for some Ni−Cu clusters containing 64, 125, 216, 343, 512, 729, 1000, and 8000 atoms using Monte Carlo simulations, and hence without a full geometry optimization. Ni−Cu clusters with $N = 55$ and 147 atoms have been studied by Montejano-Carrizales et al.[21] but also without a systematic determination of the lowest-energy structures; that is, the energies of random generated structures are simply compared to each other to find the global minimum.

Derosa et al.[39] optimized the geometry of Ni−Cu clusters, but restricted it to cluster sizes containing up to five atoms and geometries with planar configurations.

The purpose of the present work is to study systematically and in an unbiased manner both the size and the composition dependence of the total energy and the structure of a whole class of binary clusters, that is, of Ni_nCu_m clusters with N up to 20, $N = 23$, and $N = 38$ atoms. The size $N = 23$ has been chosen because of the particular stability in both cases of pure Cu and Ni clusters.[40,41] For $N = 38$, Hsu and Lai[24] found that this specific nuclearity has the consequence of driving the Cu atoms in Cu_nAu_m clusters to change dramatically the structure of the bimetallic clusters in dependence of the Cu content.

In particular, we will study whether those values of N that for the pure clusters correspond to particularly stable structures

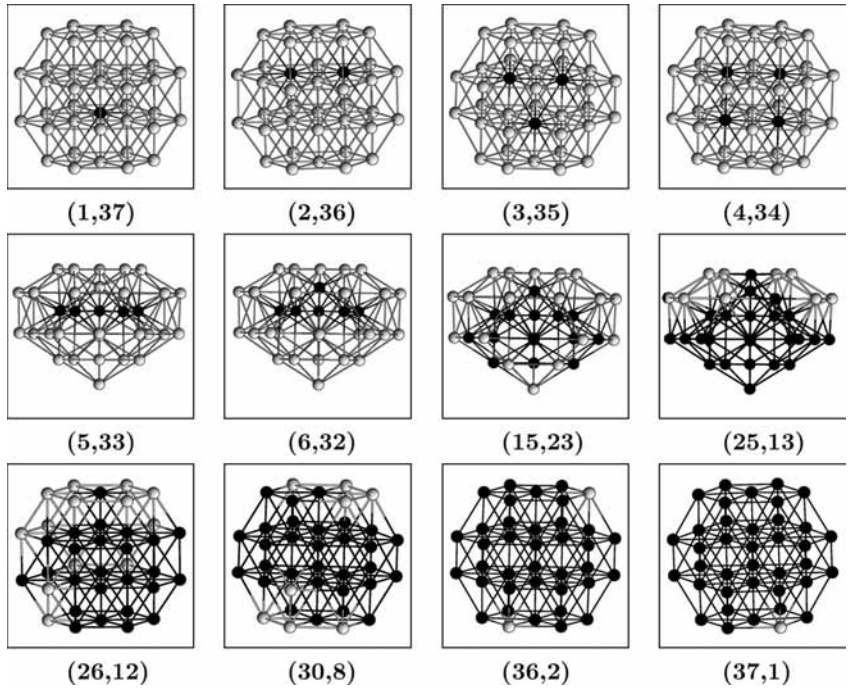

Figure 3. The energetically lowest isomers of Ni_nCu_m clusters for a fixed value of $N = 38$.

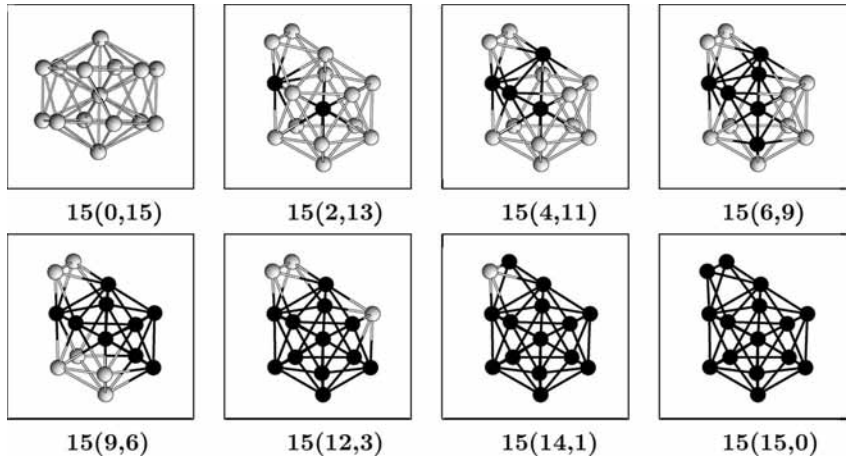

Figure 4. The energetically lowest isomers of Ni_nCu_m clusters for a fixed value of $N = 15$.

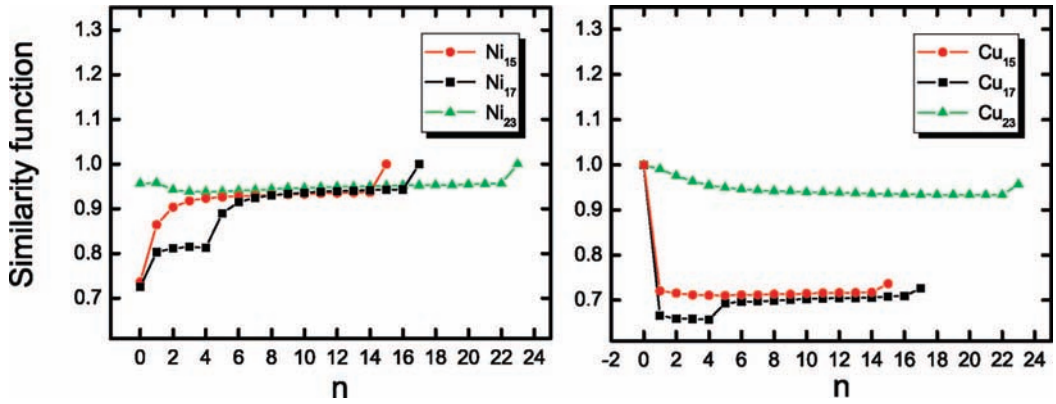

Figure 5. The similarity function vs the number of Ni atoms n. In the left panel, the structures of the bimetallic clusters of the sizes $N = 15$, 17, and 23 are compared to those of the pure Ni_{15}, Ni_{17}, and Ni_{23} clusters, respectively. The panel to the right shows the same comparison with the corresponding pure Cu clusters.

also do so in the present case. Moreover, by using various descriptors, we shall quantify to which extent the structures resemble those of the pure clusters.

Our approach is based on the embedded-atom method (EAM) for calculating the total energy of a given structure, and we use a genetic algorithm in determining the structures of the lowest

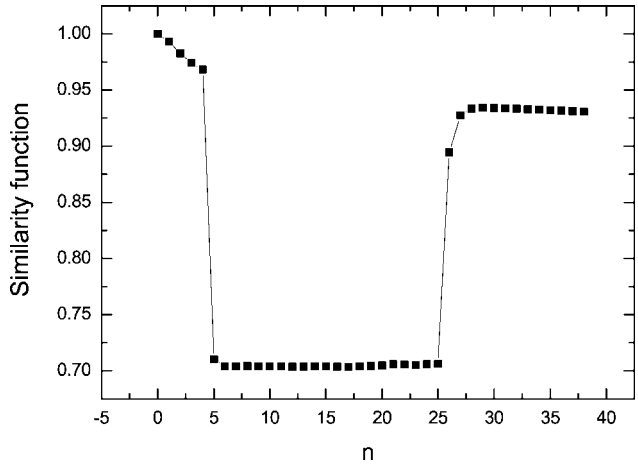

Figure 6. The similarity function vs the number of Ni atoms n. The bimetallic clusters of the size $N = 38$ are compared to those of the pure Cu_{38} clusters.

total energies. The Article is organized as follows. In section II, we briefly outline the embedded-atom method and the genetic algorithm. The main results are presented in section III, and a brief summary is offered in section IV.

II. Computational Method

A. The Embedded-Atom Method. The interactions between the atoms in the bimetallic clusters are described through the EAM in the version of Daw, Baskes, and Foiles (DBF).[42–44] The main idea of the EAM is to consider each atom as an impurity embedded in a host provided by the rest of the atoms. In addition, an electrostatic interaction between the atoms is included. Accordingly, the total energy (relative to that of the isolated atoms) has the following form

$$E_{\mathrm{tot}} = \sum_{i=1}^{N}\left[F_i(\rho_i^{\mathrm{h}}) + \frac{1}{2}\sum_{j=1(j\neq i)}^{N}\phi_{ij}(r_{ij})\right] \qquad (2)$$

In eq 2, ρ_i^{h} is the local electron density at site i, F_i is the embedding energy required to embed an atom into this density, and ϕ_{ij} is a short-range potential between atoms i and j separated by distance r_{ij}. The local density at site i is assumed being a superposition of atomic electron densities,

$$\rho_i^{\mathrm{h}} = \sum_{j=1(j\neq i)}^{N}\rho_j^{\mathrm{a}}(r_{ij}) \qquad (3)$$

where $\rho_j^{\mathrm{a}}(r_{ij})$ is the spherically averaged atomic electron density provided by atom j at the distance r_{ij}.

TABLE 1: Point Groups of the First Three Isomers

N	n,m	I	II	III	N	n,m	I	II	III	N	n,m	I	II	III	N	n,m	I	II	III
2	0,2	$D_{\infty h}$			8	7,1	C_s	C_s	C_s	12	5,7	C_s	C_s	C_s	15	3,12	C_{2v}	C_1	C_s
2	1,1	$C_{\infty h}$			8	8,0	D_{2d}	C_s	D_{3d}	12	6,6	C_s	C_{5v}	C_1	15	4,11	C_s	C_s	C_1
2	2,0	$D_{\infty h}$			9	0,9	C_{2v}	D_{3h}	C_{2v}	12	7,5	C_{5v}	C_1	C_s	15	5,10	C_{2v}	C_1	C_s
3	0,3	D_{3h}			9	1,8	C_{2v}	C_s	C_s	12	8,4	C_s	C_1	C_s	15	6,9	C_s	C_1	C_s
3	1,2	C_{2v}			9	2,7	C_s	C_s	C_1	12	9,3	C_s	C_s	C_s	15	7,8	C_1	C_s	C_1
3	2,1	C_{2v}			9	3,6	C_{2v}	C_1	C_1	12	10,2	C_s	C_s	C_s	15	8,7	C_1	C_s	C_s
3	3,0	D_{3h}			9	4,5	C_s	C_1	C_1	12	11,1	C_s	C_{5v}	C_s	15	9,6	C_1	C_{2v}	C_1
4	0,4	T_d			9	5,4	C_{2v}	C_1	C_s	12	12,0	C_{5v}	C_1	D_{3h}	15	10,5	C_s	C_1	C_s
4	1,3	C_s			9	6,3	C_1	C_s	C_1	13	0,13	I_h	C_s	C_s	15	11,4	C_s	C_2	C_1
4	2,2	C_{2v}			9	7,2	C_s	C_2	C_s	13	1,12	I_h	C_{5v}	C_s	15	12,3	C_1	C_s	C_s
4	3,1	C_{3v}			9	8,1	C_1	C_s	C_s	13	2,11	C_{5v}	D_2	C_{2v}	15	13,2	C_{2v}	C_1	C_1
4	4,0	T_d			9	9,0	C_{2v}	D_{3h}	C_{2v}	13	3,10	C_{2v}	D_{6d}	C_{2v}	15	14,1	C_s	C_1	C_s
5	0,5	D_{3h}			10	0,10	C_{3v}	D_{2h}	C_2	13	4,9	C_{3v}	C_s	C_s	15	15,0	C_{2v}	D_{6d}	C_{2v}
5	1,4	C_{2v}	C_{3v}		10	1,9	C_{3v}	C_s	C_s	13	5,8	C_{2v}	C_s	C_2	16	0,16	D_{3h}	C_s	C_s
5	2,3	C_{2v}	C_s	D_{3h}	10	2,8	C_s	C_s	C_s	13	6,7	C_s	C_s	C_1	16	1,15	C_s	C_s	D_{3h}
5	3,2	D_{3h}	C_s	C_{2v}	10	3,7	C_s	C_1	C_s	13	7,6	C_{5v}	C_2	C_{3v}	16	2,14	C_s	C_1	C_1
5	4,1	C_{3v}	C_{2v}		10	4,6	C_{3v}	C_s	C_1	13	8,5	C_s	C_s	C_s	16	3,13	C_1	C_1	C_s
5	5,0	D_{3h}			10	5,5	C_s	C_s	C_1	13	9,4	C_{2v}	C_s	C_s	16	4,12	C_1	C_1	C_1
6	0,6	O_h	C_{2v}	C_{2v}	10	6,4	C_s	C_1	C_s	13	10,3	C_{3v}	C_s	C_s	16	5,11	C_1	C_s	C_s
6	1,5	C_{4v}	C_s	C_s	10	7,3	C_{3v}	C_s	C_1	13	11,2	C_{2v}	C_{2v}	D_{5d}	16	6,10	C_1	C_1	C_1
6	2,4	C_{2v}	D_{4h}	C_{2v}	10	8,2	C_s	C_1	C_s	13	12,1	C_{5v}	I_h	C_s	16	7,9	C_1	C_1	C_s
6	3,3	C_{3v}	C_{2v}	C_s	10	9,1	C_s	C_s	C_s	13	13,0	I_h	C_s	C_s	16	8,8	C_1	C_1	C_s
6	4,2	C_{2v}	C_{2v}	D_{4h}	10	10,0	C_{3v}	D_{2h}	C_2	14	0,14	C_{3v}	C_{2v}	C_{6v}	16	9,7	C_1	C_s	C_1
6	5,1	C_{4v}	C_s	C_s	11	0,11	C_{2v}	C_2	C_{2v}	14	1,13	C_{3v}	C_{2v}	C_s	16	10,6	C_1	C_s	C_1
6	6,0	O_h	C_{2v}	C_{2v}	11	1,10	C_{2v}	C_s	C_{3v}	14	2,12	C_s	C_s	C_s	16	11,5	C_s	C_s	C_1
7	0,7	D_{5h}	C_{3v}	C_2	11	2,9	C_s	C_s	C_1	14	3,11	C_s	C_s	C_s	16	12,4	C_s	C_1	C_1
7	1,6	C_{5v}	C_{2v}	C_s	11	3,8	C_{2v}	C_1	C_{2v}	14	4,10	C_{3v}	C_s	C_1	16	13,3	C_1	C_1	C_1
7	2,5	D_{5h}	C_s	C_{2v}	11	4,7	C_s	C_s	C_1	14	5,9	C_s	C_s	C_s	16	14,2	C_s	C_1	C_1
7	3,4	C_{2v}	C_s	C_s	11	5,6	C_{2v}	C_1	C_1	14	6,8	C_1	C_s	C_1	16	15,1	C_1	C_s	C_s
7	4,3	C_{2v}	C_{2v}	C_s	11	6,5	C_1	C_s	C_s	14	7,7	C_1	C_s	C_s	16	16,0	C_s	C_s	C_2
7	5,2	C_{2v}	C_{2v}	C_s	11	7,4	C_s	C_2	C_s	14	8,6	C_s	C_1	C_1	17	0,17	T_d	C_2	C_2
7	6,1	C_{2v}	C_{5v}	C_{3v}	11	8,3	C_1	C_1	C_1	14	9,5	C_s	C_1	C_1	17	1,16	C_s	C_2	C_s
7	7,0	D_{5h}	C_{3v}	C_2	11	9,2	C_{2v}	C_1	C_s	14	10,4	C_s	C_1	C_1	17	2,15	C_s	C_s	C_1
8	0,8	D_{2d}	C_s	D_{3d}	11	10,1	C_s	C_1	C_s	14	11,3	C_1	C_s	C_s	17	3,14	C_1	C_s	C_2
8	1,7	C_s	C_s	C_s	11	11,0	C_{2v}	C_2	C_{2v}	14	12,2	C_s	C_s	C_s	17	4,13	C_s	C_1	C_s
8	2,6	C_{2v}	C_2	C_s	12	0,12	C_{5v}	C_1	D_{3h}	14	13,1	C_{3v}	C_s	C_s	17	5,12	C_2	C_s	C_s
8	3,5	C_s	C_s	C_s	12	1,11	C_{5v}	C_s	C_{5v}	14	14,0	C_{3v}	C_{2v}	C_1	17	6,11	C_1	C_1	C_1
8	4,4	D_{2d}	C_1	C_s	12	2,10	C_s	C_{5v}	C_s	15	0,15	D_{6d}	C_{2v}	D_2	17	7,10	C_2	C_1	C_1
8	5,3	C_s	C_s	C_1	12	3,9	C_s	C_s	C_s	15	1,14	C_{2v}	D_{6d}	C_s	17	8,9	C_1	C_1	C_1
8	6,2	C_{2v}	C_2	C_s	12	4,8	C_s	C_s	C_s	15	2,13	C_s	C_s	C_s	17	9,8	C_1	C_2	C_1

TABLE 2: Point Groups of the First Three Isomers

N	n,m	I	II	III	N	n,m	I	II	III	N	n,m	I	II	III	N	n,m	I	II	III
17	10,7	C_1	C_1	C_1	19	13,6	C_{5v}	C_s	C_1	23	12,11	C_1	C_1	C_1	38	28,10	C_1	C_1	C_1
17	11,6	C_2	C_1	C_1	19	14,5	C_s	C_1	C_1	23	13,10	C_1	C_1	C_1	38	29,9	C_1	C_1	C_1
17	12,5	C_1	C_1	C_1	19	15,4	C_s	C_2	C_2	23	14,9	C_s	C_s	C_1	38	30,8	C_1	C_1	C_1
17	13,4	C_2	C_2	C_s	19	16,3	C_s	C_s	C_s	23	15,8	C_1	C_1	C_1	38	31,7	C_1	C_1	C_1
17	14,3	C_1	C_{3v}	C_1	19	17,2	C_s	C_2	C_{2v}	23	16,7	C_1	C_1	C_1	38	32,6	C_s	C_1	C_1
17	15,2	C_2	C_1	C_1	19	18,1	C_s	C_{5v}	C_{2v}	23	17,6	C_s	C_s	C_1	38	33,5	C_1	C_1	C_1
17	16,1	C_1	C_s	C_1	19	19,0	D_{5h}	C_1	C_s	23	18,5	C_1	C_1	C_1	38	34,4	C_2	C_1	C_1
17	17,0	C_2	C_s	C_s	20	0,20	C_{2v}	D_{3d}	D_2	23	19,4	C_{2v}	C_1	C_1	38	35,3	C_1	C_1	C_1
18	0,18	C_s	C_{5v}	C_{2v}	20	1,19	C_s	C_{3v}	C_2	23	20,3	C_s	C_1	C_1	38	36,2	D_2	C_1	C_s
18	1,17	C_s	C_s	C_s	20	2,18	C_{2v}	D_{3d}	D_2	23	21,2	C_1	C_{2v}	C_s	38	37,1	C_s	C_s	C_1
18	2,16	C_s	C_{5v}	C_1	20	3,17	C_s	C_{2v}	C_s	23	22,1	C_s	C_s	C_1	38	38,0	O_h	C_{5v}	C_{5v}
18	3,15	C_1	C_1	C_1	20	4,16	C_{2v}	C_s	C_s	23	23,0	D_{3h}	D_{3h}	D_2					
18	4,14	C_1	C_s	C_s	20	5,15	C_s	C_{2v}	C_s	38	0,38	O_h	C_5	C_5					
18	5,13	C_s	C_s	C_1	20	6,14	C_s	C_{2v}	C_1	38	1,37	C_{4v}	C_1	C_5					
18	6,12	C_1	C_s	C_s	20	7,13	C_{2v}	C_s	C_s	38	2,36	C_{2v}	C_1	C_1					
18	7,11	C_s	C_1	C_s	20	8,12	C_s	C_s	C_2	38	3,35	C_{3v}	D_2	C_1					
18	8,10	C_1	C_1	C_1	20	9,11	C_{2v}	C_1	C_1	38	4,34	D_{4h}	C_1	C_1					
18	9,9	C_s	C_s	C_s	20	10,10	C_1	C_1	C_s	38	5,33	C_{5v}	C_1	C_1					
18	10,8	C_s	C_s	C_s	20	11,9	C_1	C_s	C_2	38	6,32	C_{5v}	C_5	C_5					
18	11,7	C_s	C_s	C_s	20	12,8	C_1	C_1	C_s	38	7,31	C_{5v}	C_1	C_3					
18	12,6	C_1	C_s	C_1	20	13,7	C_1	C_1	C_1	38	8,30	C_s	C_3	C_1					
18	13,5	C_s	C_1	C_1	20	14,6	C_1	C_1	C_1	38	9,29	C_s	C_s	C_s					
18	14,4	C_s	C_1	C_1	20	15,5	C_1	C_1	C_1	38	10,28	C_s	C_1	C_s					
18	15,3	C_s	C_s	C_1	20	16,4	C_1	C_s	C_1	38	11,27	C_s	C_1	C_1					
18	16,2	C_s	C_1	C_1	20	17,3	C_2	C_s	C_1	38	12,26	C_{5v}	C_1	C_1					
18	17,1	C_1	C_s	C_1	20	18,2	C_1	C_1	C_s	38	13,25	C_s	C_1	C_1					
18	18,0	C_s	C_{5v}	C_s	20	19,1	D_2	C_1	C_1	38	14,24	C_s	C_s	C_s					
19	0,19	D_{5h}	C_1	C_1	20	20,0	C_{2v}	D_{3d}	D_2	38	15,23	C_s	C_1	C_1					
19	1,18	C_{5v}	C_{2v}	C_{5v}	23	0,23	D_{3h}	D_2	D_{3h}	38	16,22	C_s	C_s	C_1					
19	2,17	D_{5h}	C_s	C_{5v}	23	1,22	C_{2v}	C_{3v}	C_1	38	17,21	C_{5v}	C_1	C_1					
19	3,16	C_{2v}	C_{5v}	C_s	23	2,21	C_{2v}	C_1	C_s	38	18,20	C_s	C_1	C_1					
19	4,15	C_{2v}	C_{2v}	C_s	23	3,20	D_{3h}	C_s	C_s	38	19,19	C_s	C_1	C_1					
19	5,14	C_{2v}	C_{2v}	C_s	23	4,19	C_{3v}	C_s	C_{2v}	38	20,18	C_s	C_1	C_1					
19	6,13	C_{2v}	C_1	C_1	23	5,18	C_s	C_s	C_{2v}	38	21,17	C_1	C_1	C_1					
19	7,12	D_{5h}	C_1	C_s	23	6,17	C_s	C_s	C_s	38	22,16	C_{5v}	C_1	C_1					
19	8,11	C_s	C_1	C_2	23	7,16	C_{2v}	C_2	C_1	38	23,15	C_{5v}	C_s	C_1					
19	9,10	C_s	C_2	C_2	23	8,15	C_1	C_s	C_1	38	24,14	C_1	C_1	C_1					
19	10,9	C_s	C_s	C_s	23	9,14	C_2	C_1	C_1	38	25,13	C_1	C_1	C_1					
19	11,8	C_s	C_2	C_2	23	10,13	C_s	C_1	C_1	38	26,12	C_1	C_1	C_1					
19	12,7	C_s	C_1	C_1	23	11,12	C_1	C_1	C_1	38	27,11	C_1	C_1	C_1					

The detailed analysis made in ref 44 has shown that the main Ansatz of the EAM, eq 2, also holds good in the case of the binary alloys. In accord with ref 44, the pair interaction between two different species (A−B/B−A heterointeraction) can be approximated by the geometric mean of the pair interaction for the individual species: $\phi_{AB}(R) = \sqrt{(\phi_{AA}(R)\cdot\phi_{BB}(R))}$. Daw, Baskes, and Foiles determined the embedding functions for the Ni−Cu system empirically by fitting to experimental data of bulk sublimation energy, elastic constant, and the heat of solution of binary alloys.[44] The values for ρ_i^a, F_i, and ϕ_{ij} are available in numerical form for Ni and Cu.[45] The validity of the embedding functions for the Ni−Cu system has been tested by computing a wide range of properties as, for example, the segregation energy of substitutional impurities to the (100) surface.[44]

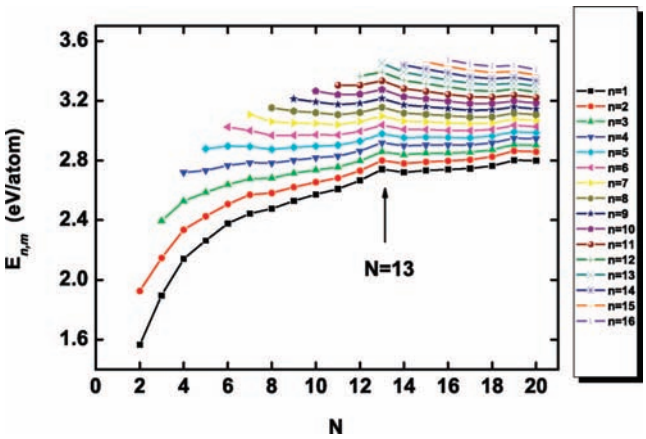

Figure 7. The binding energy per atom as a function of cluster size for different number of Ni atoms *n*.

The EAM has been successfully applied to many bulk and low-symmetric problems in transition metals such as defects, surface structures, and surface segregation/mixing effects in alloys.[46] Furthermore, in our previous works[40,41,47–49] (those include also the discussions with the available experiments), we found that this approach provides accurate information on pure Cu_N and Ni_N clusters, which is our main reason for choosing this potential for studying Ni_nCu_m clusters.

Considering two types of atoms A (Ni) and B (Cu), we have adopted for the case of computational convenience that all of the A-atoms have in eq 2 the numbers between 1 and N^A and the B-atoms have numbers between $N^A + 1$ and $N = N^A + N^B$. Further, there are two different cutting distances at which three different types of short-range interactions, A−A, B−B (homointeractions), and A−B/B−A (heterointeractions), vanish (see ref 45): $r_{cut}^{Ni} = 4.80$ Å for A−A interaction and $r_{cut}^{Cu} = 4.95$ Å for B−B interaction. The cutting distance for the A−B/B−A

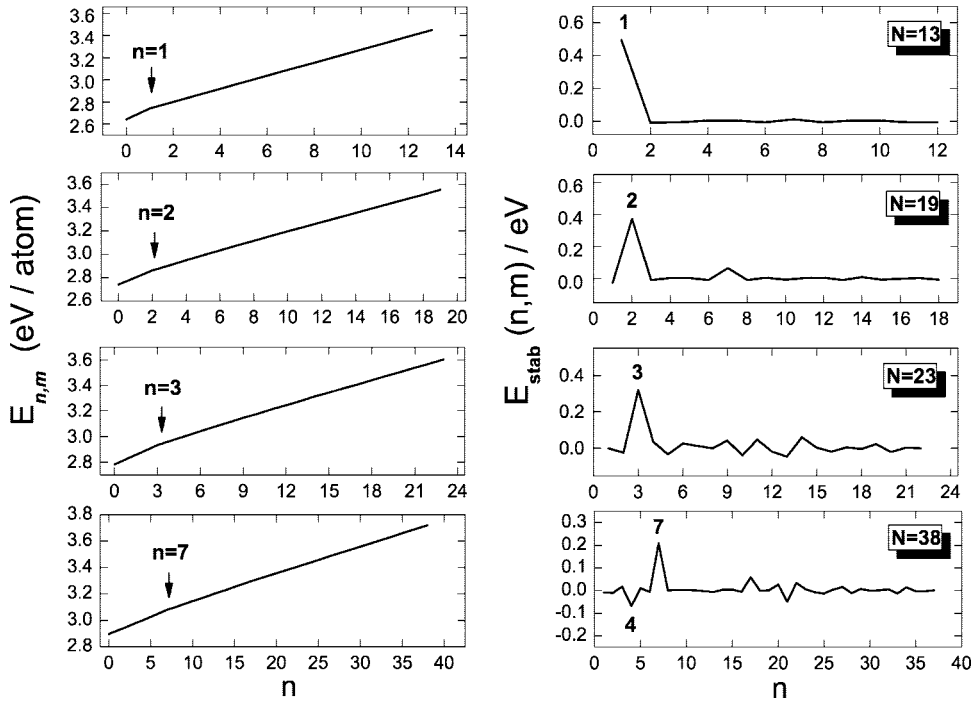

Figure 8. The left panels show the binding energy per atom and the right panels the stability energy $E_{stab}(n, m)$ as a function of n for $N = n + m$ being 13 (top panels), 19 and 23 (middle panels), and 38 (bottom panels).

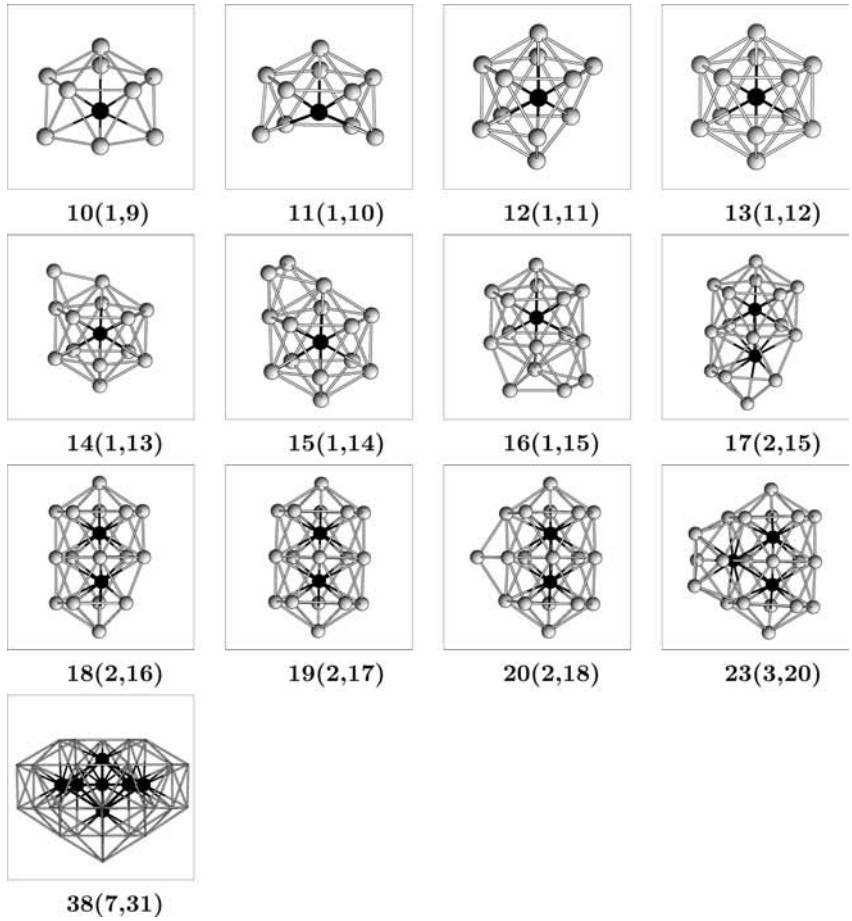

Figure 9. The structures of the magic Ni_nCu_m clusters for $10 \leq N \leq 20$, $N = 23$, and $N = 38$ atoms. The labels are given as $N(n, m)$ with N being the total number of atoms, n the number of Ni atoms, and m the number of Cu atoms.

heterointeractions is the minimum from these two distances or 4.80 Å. Correspondingly, the neighbor analysis in the case of bimetallic clusters is more complicated than that for monatomic ones. For each pair of atoms i, j, the following situations are possible: (i) $r_{ij} \geq r_{cut}^{Cu}$, no interactions and no contributions of electron density at sites i and j; (ii) $r_{ij} \leq r_{cut}^{Ni}$, the atoms interact

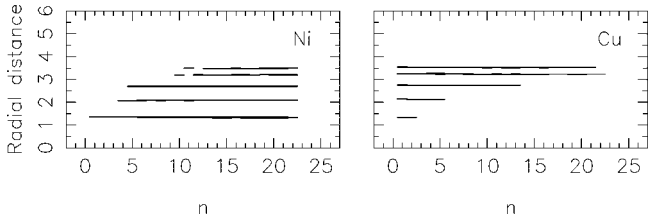

Figure 10. The radial distances (in Å) for Ni and Cu atoms, separately, as a function of the number of Ni atoms, n. In each panel, a small horizontal line shows that at least one atom of the corresponding type has that distance to the center of the cluster for a given value of $N = 23$.

with each other, i contributes electron density at site j and j contributes at site i; (iii) $r_{cut}^{Ni} < r_{ij} < r_{cut}^{Cu}$, i = Ni, j = Ni, as in case (i); (iv) $r_{cut}^{Ni} < r_{ij} < r_{cut}^{Cu}$, i = Cu, j = Cu, as in case (ii); (v) $r_{cut}^{Ni} < r_{ij} < r_{cut}^{Cu}$, i = Ni, j = Cu, no interactions between atoms, atom j contributes electron density at site i, contribution to the total energy [eq 2] via the embedding function $F_i(\rho_i^h)$; and (vi) $r_{cut}^{Ni} < r_{ij} < r_{cut}^{Cu}$, i = Cu, j = Ni, no interactions between atoms, atom i contributes electron density at site j, contribution to the total energy [eq 2] via the embedding function $F_j(\rho_j^h)$. We emphasize that our approach is consistent with that of the original EAM method.

B. The Genetic Algorithm. The global minima of the total energy of the binary clusters have been determined using the variable metric/quasi-Newton method in combination with a genetic algorithm.

Genetic algorithms[50,51] are optimization techniques based on the mechanisms of natural selection. Our version of the genetic algorithms has been applied to clusters with one, two, and three types of atoms, for example, Au, Na, AlO, and HAlO clusters,[52–55] and we have found that this optimization method is reliable when studying the structural and energetic properties of one-component as well as of multicomponent clusters.

In the present study on a given Ni_nCu_m cluster, a number of randomly generated structures are optimized locally with the quasi-Newton method. The three lowest-total-energy structures are then used as the initial population. Subsequently, a new set of clusters is constructed by cutting each of the three original ones randomly into two parts, which are interchanged and randomly rotated relative to each other, and afterward allowing them to relax. Out of the total set of six structures, the three with the lowest total energy are kept as the next generation. This procedure is repeated until the lowest total energy is unchanged for a large number of generations.

III. Results

A. Structural Properties. Whereas macroscopic, crystalline Cu and Ni have the same crystal structures (fcc), pure copper and nickel clusters, Cu_N and Ni_N, have different structures for certain values of N. For $2 \le N \le 14$, $18 \le N \le 20$, and $N = 23$, the clusters have the same lowest-energy-minimum structures, whereas for $15 \le N \le 17$ they possess different ground-state structures. For instance, for N = 3, 4, 5, and 6, the optimized structures correspond to an equilateral triangle, a

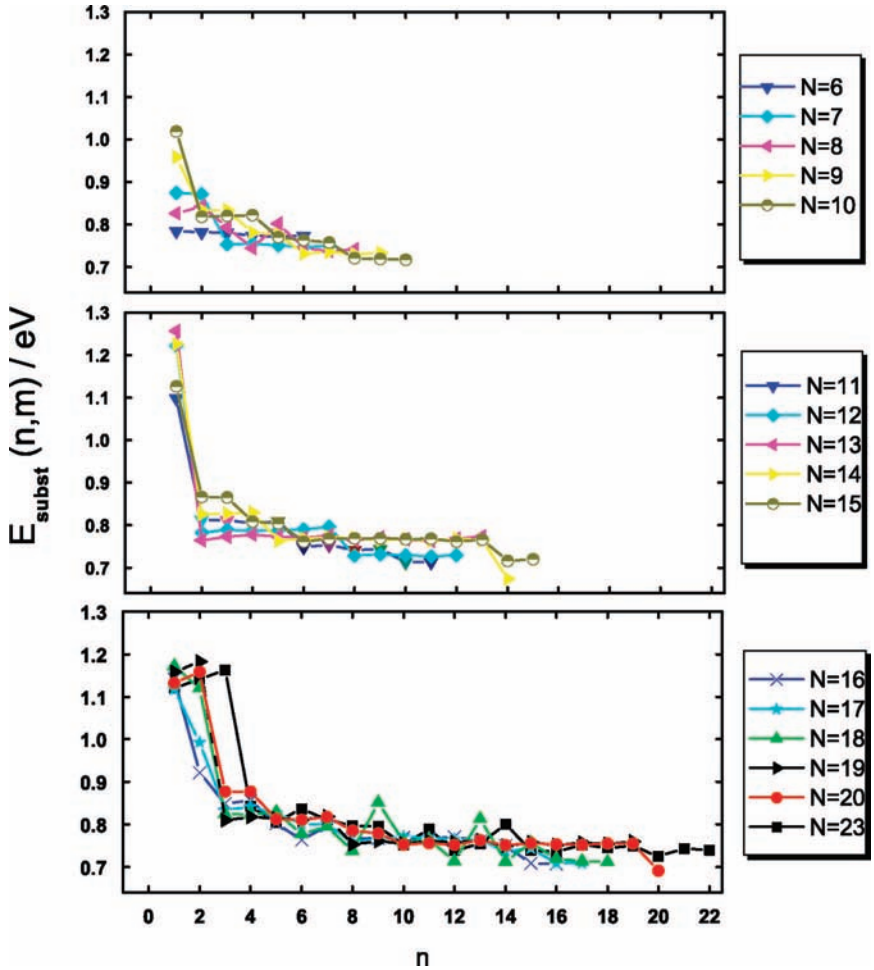

Figure 11. The total-energy difference between a cluster with n Ni atoms and a cluster with one less Ni atom and one more Cu atom as a function of n for different cluster sizes N.

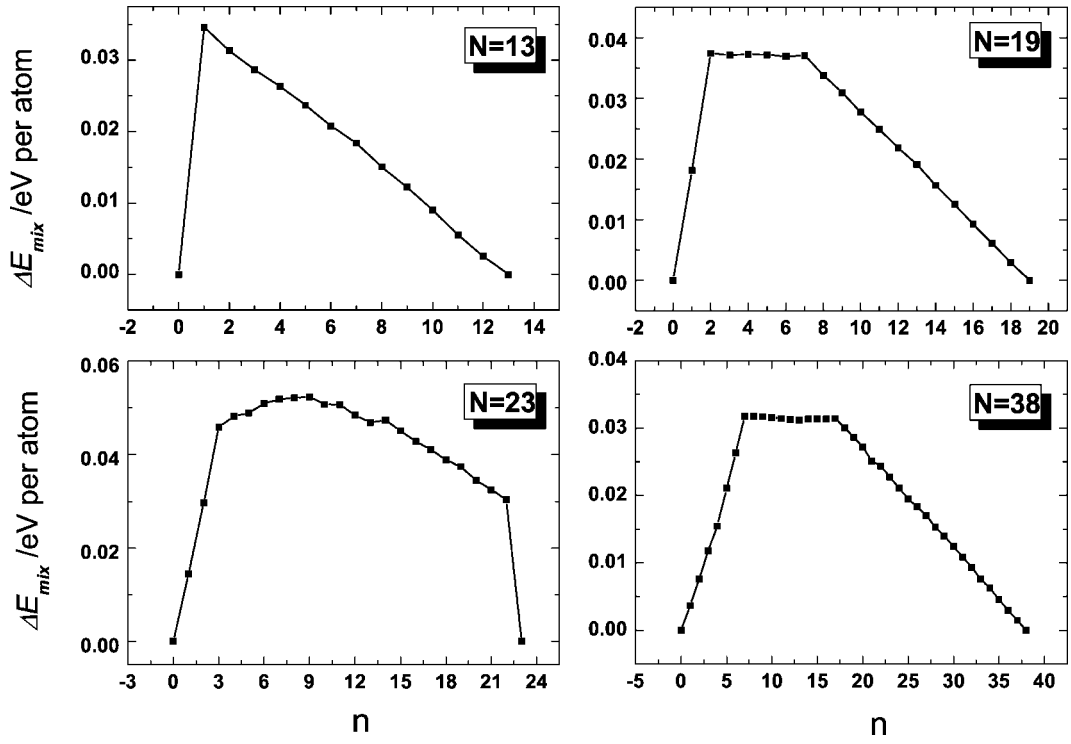

Figure 12. ΔE_{mix} as a function of n for $N = 13$, 19, 23, and 38.

tetrahedron, a trigonal bipyramid, and an octahedron, respectively, whereas for $N = 15$ a centered bicapped hexagonal antiprism (D_{6d}) is found for Cu, but a bicapped icosahedron (C_{2v}) is found for Ni.[40,41] Thus, an important issue is whether these structures will be recovered for the bimetallic clusters, and, for $15 \leq N \leq 17$, which (if any) of the two structures for the pure clusters will be found.

In Figures 1 and 2, we show the global-minimum structures of monometallic and bimetallic clusters for $N = 13$ and $N = 23$ for different values of (n, m). The results are typical for most of the clusters we have examined; that is, the geometry of the clusters is the same as that found for both pure clusters. Moreover, Ni atoms (dark atoms) tend to occupy the central parts of the clusters, whereas Cu atoms are often found on the surface.

A different scenario concerning the evolution of the structure with composition is observed when looking at alloy clusters of $N = 38$ (see Figure 3). Up to $n = 4$, the lowest-energy structure of the pure clusters, the truncated octahedron, is also found for the bimetallic clusters. Yet from $n = 5$ upward there is a dramatic change to a structure with pentagonal symmetry (C_{5v}), presenting an icosahedral fragment. In this structure, the nearest Ni−Ni distance is 3% shorter than that in the octahedral structure with 4 Ni atoms. Thus, for the Ni atoms, which possess the higher cohesive energy ($E_{\mathrm{coh}}^{\mathrm{Ni}} = 4.44$ eV, $E_{\mathrm{coh}}^{\mathrm{Cu}} = 3.49$ eV),[56] the possibility is given to form stronger bonds with the corresponding lowering of the cluster total energy. In the composition range $n = 26-37$, we find again the octahedral symmetry. The structural evolution with declining atom fraction of Cu described above is quite different from the structural change of the Cu_nAu_m clusters (with $n + m = 38$) in a study of Hsu and Lai.[24] In the mentioned study, the authors classify four categories of the lowest-energy structures: octahedral, pentagonal, hexagonal, and amorphous.

Next, we consider the case of $N = 15$ for which the pure clusters have different ground-state structures. Here, one may expect that the bimetallic clusters of this size would have Cu-like or Ni-like ground-state structures for low nickel and low copper concentrations, respectively. However, as Figure 4 shows, all structures of these Ni_nCu_m clusters with $n \neq 0$ prefer the structure of the pure Ni cluster (C_{2v}) over that of the pure Cu cluster (D_{6d}). The same trend is found for the 16-atom bimetallic clusters, which are not shown here. These two examples suggest that the structural properties of the Ni−Cu alloy clusters can not be obtained by interpolating (as a function of concentration) between the properties of the corresponding pure clusters.

To obtain a quantitative comparison of the structures of the bimetallic clusters with those of the pure Cu and Ni clusters of the same sizes, we use the so-called similarity functions that we have used in previous studies, too.[40,41] For each atom, we define its radial distance

$$r_n = |\vec{R}_{\mathrm{n}} - \vec{R}_0| \tag{4}$$

with

$$\vec{R}_0 = \frac{1}{N}\sum_{i=1}^{N} \vec{R}_{\mathrm{i}} \tag{5}$$

These are sorted in increasing order. Simultaneously, for each of the pure clusters we calculate and sort the radial distances, $\{r_n'\}$, for this, too. Subsequently, from

$$q = \left[\frac{1}{N}\sum_{n=1}^{N} (r_n - r_n')^2\right]^{1/2} \tag{6}$$

the similarity function is given as

$$S = \frac{1}{1 + q/u_{\mathrm{l}}} \tag{7}$$

($u_{\mathrm{l}} = 1$ Å), which approaches 1 (0) if the A_nB_m cluster is very similar to (different from) the pure cluster. The results are shown in Figure 5for $N = 15$, 17, and 23 and in Figure 6 for $N = 38$ as a function of the number of Ni atoms, n. The results for

$N = 23$ are typical for most values of N; that is, the structure is very similar to that of the pure clusters. The main difference can be related to the differences in Ni−Ni, Cu−Cu, and Ni−Cu bond lengths.

Different results are found for $N = 15$ and $N = 17$. For these cluster sizes, the calculated functions show a higher similarity of the bimetallic clusters to the structure of the pure Ni_N cluster than to that of the pure Cu_N cluster. For $N = 17$, an additional discontinuity in the similarity functions at $n = 5$ indicates the formation of new structures, different from those of the pure Ni and Cu clusters. The similarity function for $N = 38$ in Figure 6 shows the structural change in the composition range $n = 5-25$, discussed for Figure 3. Up to $n = 4$ and from $n = 26$ upward, the lowest-energy structure for the bimetallic clusters is found to be the truncated octahedron (the same as for the pure clusters). Yet from $n = 5$ to $n = 25$, there is a change to a structure with pentagonal symmetry C_{5v}, very different from the pure Ni and Cu clusters.

As mentioned above, we found that for $9 \leq N \leq 20$ the central position of the global-minimum structures, which are icosahedral, is always occupied by a Ni atom (see, for example, Figures 1 and 4). There are three possible reasons for that. First, it is well-known that there is strong internal strain in an icosahedron. Replacing the inner atom with smaller atoms (in our case Cu atoms with smaller Ni ones) may decrease this strain significantly. Second, Ni−Ni bonds are stronger, making structures with large Ni coordinations energetic favorable. Third, Cu possesses a smaller surface energy [$\sigma(111) = 69.5$ kJ/mol], as compared to that of Ni [$\sigma(111) = 80$ kJ/mol] (see, for example, ref 57), once again suggesting that Ni atoms prefer to occupy positions with the highest coordination numbers (e.g., the center of an icosahedron).

In agreement with our findings, Montejano-Carrizales et al.[21] explained the surface segregation of Cu by the smaller surface energy of Cu as compared to Ni. Also, Bailey et al.[26] observed a correlation between cohesive energy, surface energy, and the atomic size on the one side and the structure of bimetallic Ni−Al clusters with up to 55 atoms on the other side. They found that the central site of the cluster is favored by the Ni atom because of its smaller size and higher cohesive and surface energies. The results of Lordeiro et al.,[8] López et al.,[23] Hsu and Lai,[24] and Cheng et al.[25] on Cu−Au clusters, who observed the tendency of the smaller atom (Cu) to occupy the central site of the icosahedron and of the larger atom (Au) to locate at surface sites, are similar to our findings, too. Thus, our results are in agreement with those of the earlier studies on other, but related, systems.

On the other hand, the icosahedral structures with only one Au atom found by Lordeiro et al.[8] is markedly different from those with one Cu atom found by us. Whereas in all global-minimum structures determined in our study the central position of the icosahedron is always occupied by the atom with the higher surface energy and the slightly smaller size (Ni), the central atom in the work of Lordeiro et al.[8] can be replaced by a Au atom. Obviously, the fact that Au atoms possess a lower surface energy and larger size than Cu atoms does not necessarily drive them to locate at the surface. The crucial factor for the atomic arrangement in Cu−Au clusters is that Au−Cu bonds are stronger than Cu−Cu bonds (Au−Au > Au−Cu > Cu−Cu),[58] which drives the single Au atom to maximize the interactions with atoms of the different type. This competition between maximizing the strongest atomic interactions and minimizing the bulk strain that exists in a Cu−Au icosahedron is not to be found in a Ni−Cu cluster, resulting in different homotops of the icosahedral structures of both cluster types.

Besides, the fact that the central atom of a Cu−Au icosahedron prefers to be surrounded by atoms of different type can be explained by the negative heats of solution[58] for solid Cu−Au alloys favoring mixing of atoms of a different type, whereas the positive heats of solution of Ni−Cu alloys lead to a segregation of copper to the surface. This segregation tendency combined with the role of the relative cohesive energies results in different structures as compared to Cu−Au clusters despite the relative similar behavior in size and surface energy of the atoms.

In Tables 1 and 2, we list the point groups of the three energetically lowest isomers for the clusters investigated in this work. One can identify a symmetry reduction from I_h to C_{5v} when going from the first to the second isomer in the case of Ni_1Cu_{12}, whereas for $Ni_{12}Cu_1$ there is an increase in symmetry from C_{5v} to I_h. The reason is that, in contrast to the first isomers of these bimetallic clusters, the second isomers have a Cu atom and not a Ni atom at the center. The energy difference between the first and the second isomers for these clusters is rather large, that is, 0.51 eV for Ni_1Cu_{12} and 0.62 eV for $Ni_{12}Cu_1$. Thus, also this finding demonstrates that when Ni atom is occupying the center a strong stabilization of the icosahedral structure results.

When comparing with the energy difference between the first and the second isomers of the pure copper (1.06 eV) and the pure nickel (1.16 eV) cluster, the energy differences mentioned above are smaller. The reason is that for bimetallic clusters these isomers are homotops and the existence of homotops leads to a much richer total-energy surface.

B. Energetic Properties. Next, we shall turn our attention to the energetic properties and stability of the Ni−Cu bimetallic clusters as a function of cluster size and composition. In Figure 7, we show the binding energy per atom

$$E_{n,m} = -E_{tot}(n, m)/N \quad (8)$$

as a function of cluster size for $n = 1-16$. Here, $E_{tot}(n, m)$ is the total energy of the energetically lowest Ni_nCu_m cluster. A kink at $N = 13$ and a smaller one at $N = 19$ indicate a stabilization of the structures at these cluster sizes for all Ni concentrations due to the icosahedral geometry. Thus, structures that are particularly stable for the monatomic clusters due to geometric effects may also be so for bimetallic clusters. Another relevant observation is that for $N = 15$, 16, and 17 the binding energy increases for clusters containing up to $n = 4$ Ni atoms and decreases for clusters containing $n = 6$ Ni atoms upward. The same result, that the concentration effect on the binding energy is more important than the geometrical one, is also found for $N = 10$ and $N = 11$. Further, we could find the nonmonotonic dependence of the binding energy $E_{n,m}$ with increasing N in the range $n \leq N \leq 13$ for $n = 4-10$. Those regions are especially pronounced for $n = 6$, 7, and 8 (see Figure 7). Next, we use

$$E_{stab}(n, m) = E_{tot}(n + 1, m - 1) + E_{tot}(n - 1, m + 1) - 2E_{tot}(n, m) \quad (9)$$

to check the relative stability of a cluster as compared to clusters of the same size containing one more and one less Ni atom. As a function of n for given N, E_{stab} has peaks at particularly stable clusters, so-called magic clusters. We notice that if the substitution of a Ni atom by a Cu atom was accompanied by a concentration- and size-independent total-energy difference, E_{stab} would vanish.

In Figure 8, we show this function together with the binding energy, for four different values of N, that is, $N = 13$, 19, 23, and 38. We observe that the pure Ni clusters possess the most stable structures (if compared to bimetallic clusters of the same size) for all investigated cluster sizes. Further, among the bimetallic Ni−Cu clusters, the $Ni_{N-1}Cu_1$ clusters have the lowest total energy and hence are the most stable ones in the size range $N = 2-20$. This is not surprising as the binding energy is expected to increase with Ni content due to its higher cohesion.

The plots show special features, that is, a kink in the binding energy function and a maximum in the stability function $E_{stab}(n, m)$, for $n = 1$, 2, 3, and 7. The corresponding magic clusters for a larger set of values of N are presented in Figure 9. The maximum in the stability function at $n = 1$ for $N = 13$ refers to the icosahedron with only one Ni atom at the center, whereas for $n = 2$ and $N = 19$ the double icosahedron with two Ni atoms centered in each icosahedron is found. These two structures turn out to be especially stable because they are obtained both from the size dependence of the binding energy as well as from the concentration dependence of the stability function (see also Figure 8). In our study, the magic cluster for the size $N = 38$ refers to the structure with Ni atoms forming a pentagonal bipyramid in the cluster core. For comparison, we want to mention that in a study of Hsu and Lai[24] of Cu−Au clusters the peak in the stability function for $N = 38$ is found to be at $n = 6$. In the corresponding magic cluster, the Cu atoms form a plane hexagon at the center of the cluster.

Further, Figure 9 shows that all of the magic clusters in the size range $10 \leq N \leq 20$ have icosahedron-based structures with a Ni atom at the center of each icosahedron. The magic cluster for $N = 23$ is a triple icosahedron, and it shows a perfect core−shell structure. The Ni atoms centered in each icosahedron form the core, while the copper atoms, which possess the lower surface energy, form the shell of the cluster. That there is a tendency toward the formation of core−shell structures can be further demonstrated by plotting the radial distances of the Ni and Cu atoms separately. This is done in Figure 10 for $N = 23$. For a small concentration of nickel (until $n = 3$), the Ni atoms prefer to occupy the inner positions, whereas with increasing concentration of nickel, they have to occupy positions further away from the center, but first for $n = 11$ also surface positions are occupied by Ni. The Cu atoms display the opposite behavior: for a small copper concentration they are located to the surface region, and with increasing concentration of Cu, also the inner positions of the cluster are occupied.

The quantity

$$E_{subst}(n, m) = E_{tot}(n - 1, m + 1) - E_{tot}(n, m) \qquad (10)$$

describes the relative stability of a cluster with n Ni atoms with respect to clusters with one less Ni and one more Cu atom. Thus, the function represents the energy gain (or loss) when a Cu atom is replaced by a Ni atom. In Figure 11, this function is presented in dependence of the number of n for different cluster sizes, $N = n + m$. For $n = 1$ and N up to 8 the function has relatively low values because the pure Cu clusters of these sizes do not form strained icosahedral structures that can be stabilized by the replacement of a centered Cu atom by a smaller Ni atom. From $N = 9$ upward, the stabilization effect begins to increase, corresponding to the icosahedral growth of the clusters (cf., Figure 9). In agreement with the discussion above, the most pronounced peak is found for $N = 13$ and $n = 1$, describing the strong tendency of a Ni atom to replace one Cu atom in the center of the icosahedron. The peaks for the other two magic clusters at $n = 2$ for $N = 19$ and at $n = 3$ for $N = 23$ possess slightly lower values. Obviously a replacement of a Cu atom centered in the second icosahedron of a double icosahedron leads to a lower stabilization of the structure as compared to the replacement of a Cu atom centered in a single icosahedron. The reason is that by the replacement of the Cu atom by the smaller Ni atom in the center of the first icosahedron a major part of the strain is released. Thus, when the second Ni atom is added it will occupy a position at the center of a less strained icosahedron.

Another criterion that we use for comparing the relative stability of alloy clusters of the same size but with a different composition is the change in cluster binding energy on mixing defined by:[59]

$$\Delta E_{mix} = E_{n,m}^{Ni-Cu} - \frac{m}{N}E_N^{Cu} - \frac{n}{N}E_N^{Ni} \qquad (11)$$

where $E_{n,m}^{Ni-Cu}$ is the binding energy of the alloy cluster containing n Ni atoms, m is the number of the Cu atoms in the cluster, and $E_N^{Cu}(E_N^{Ni})$ is the cohesive energy of the pure $Cu_N(Ni_N)$ cluster. The function represents the energy gain (or loss) for a mixed cluster with respect to pure clusters of the same size. Here, we want to emphasize that in our study positive values for the mixing energies refer to exothermic process. Thus, a positive value corresponds to a nanoalloy cluster, which is thermodynamically stable with respect to corresponding pure elemental clusters. The energies of mixing of the energetically lowest isomers for each composition are shown in Figure 12 for the nuclearities $N = 13$, 19, 23, and 38. The mixing energy for all bimetallic clusters investigated here is found to be positive, corresponding to energy-favored mixing. These results are not consistent with the endothermic experimental enthalpy of mixing in solid Ni−Cu alloys,[58] which favors ensembles with neighbors of the same type. We deduce that in contrast to bulk Ni−Cu alloys the formation of Ni−Cu nanoalloy clusters is energetically favored.

It is also interesting to observe that for $N = 19$ and 38 there is a well-defined composition range: from $n = 2$ to 7 and from $n = 7$ to 17 (with a maximum value at $n = 9$) where the structures possess a remarkable stability. This result suggests that beside the perfect core−shell structures with all Cu atoms on the surface and all Ni atoms inside, there is a range of very stable bimetallic structures with Ni atoms occupying both the core and the surface. For $N = 23$, this range begins from $n = 3$ and it is less pronounced, whereas for $N = 13$, there is only one structure at $n = 1$ with special stability relative to the corresponding pure clusters.

To sum, our calculations on small Ni−Cu clusters confirm the tendency for segregation of Cu to the surface, predicted by experiments[33−35] and theoretical[60,61] calculations for Ni−Cu macroscopic alloys as well as by Monte Carlo simulations[37,38] for larger Ni−Cu clusters (64−8000 atoms). This effect is explained by the difference in the cohesive and surface energies of Cu and Ni, by the bond enthalpy of the Ni−Cu bond, which is smaller than the average of those of Ni−Ni and Cu−Cu bonds,[58] and by the positive heats of mixing of solid Ni−Cu alloys.[58]

IV. Conclusions

In this work, we have studied the structural and energetic properties of Ni_nCu_m bimetallic clusters with $N = n + m$ up to 20 atoms and additionally for $N = 23$ and 38 atoms. We have investigated systematically and unbiased both the size and the composition dependence of the total energy and the structure of the clusters. The total energy of the bimetallic clusters was

computed with the embedded-atom method in the version of Daw, Baskes, and Foiles. The global geometry optimization was performed using a genetic algorithm.

We have determined the lowest-energy structures as well as the magic clusters for all considered cluster sizes and concentrations of the components. It is demonstrated that all Ni−Cu clusters investigated in this work are energetically stable. Comparing bimetallic clusters with homoatomic clusters of the same size, we found that the most stable clusters for each cluster size are those composed of Ni atoms, due to their higher cohesive energy. Among the bimetallic clusters in the size range $N = 2-20$, the $Ni_{N-1}Cu_1$ clusters possess the highest stability.

Furthermore, our results show that an icosahedron, a double icosahedron, and a triple icosahedron with one, two, and three Ni atoms, respectively, are especially stable (magic). Thus, structures that for the pure clusters are particularly stable are also so for the bimetallic clusters. In addition, it is found that for all global-minimum structures of the Ni−Cu bimetallic clusters Ni atoms occupy mainly high-coordination inner (core) sites. In contrast, Cu atoms show a tendency to occupy lower-coordination sites on the cluster surface.

Moreover, we found that most of the bimetallic cluster structures have geometries similar to those of pure Ni clusters. The size $N = 38$ presents a special case: from $n = 5$ upward the bimetallic clusters undergo a dramatic structural change from the truncated octahedron to a structure with pentagonal symmetry and return at $n = 25$ again to the octahedral symmetry.

Finally, in contrast to the bulk, the ground-state structures of Ni_nCu_{15-n}, Ni_nCu_{16-n}, and Ni_nCu_{17-n} clusters do not experience a smooth transition between the structures of pure copper and pure nickel clusters as the number of Ni atoms changes. For these sizes, the concentration effect on energy turned out to be more important than the geometric effect.

Acknowledgment. This work was supported by the DFG through the project Sp 439/24-1.

References and Notes

(1) Qi, W. H.; Wang, M. P. *J. Mater. Sci. Lett.* **2002**, *21*, 1743.
(2) Balleto, F.; Ferrando, R. *Rev. Mod. Phys.* **2005**, *77*, 371.
(3) Balamurugan, B.; Maruyama, T. *Appl. Phys. Lett.* **2005**, *87*, 143105.
(4) Gaudry, M.; Cottancin, E.; Pellarin, M.; Lerme, J.; Arnaud, L.; Huntzinger, J. R.; Vialle, J. L.; Broyer, M.; Rousset, J. L.; Treilleux, M.; Melinon, P. *Phys. Rev. B* **2003**, *67*, 155409.
(5) Xiao, S.; Hu, W.; Luo, W.; Wu, Y.; Li, X.; Deng, H. *Eur. Phys. J.* **2006**, *54*, 479.
(6) Aguado, A.; Gonzalez, L. E.; Lopez, J. M. *J. Phys. Chem. B* **2004**, *108*, 11722.
(7) Mottet, C.; Rossi, G.; Balleto, F.; Ferrando, R. *Phys. Rev. Lett.* **2005**, *95*, 035501.
(8) Lordeiro, R. A.; Guimares, F. F.; Belchoir, J. C.; Johnston, R. L. *Int. J. Quantum Chem.* **2003**, *95*, 112.
(9) Lloyd, L. D.; Johnston, R. L.; Salhi, S.; Wilson, N. T. *J. Mater. Chem.* **2004**, *14*, 1691.
(10) Wang, J.; Wang, G.; Chen, X.; Lu, W.; Zhao, J. *Phys. Rev. B* **2002**, *66*, 014419.
(11) Sun, X.; Toledo, J. A.; Cui, Z. L.; Zhang, Z. K. *J. Nanopart. Res.* **2001**, *3*, 325.
(12) Baletto, F.; Mottet, C.; Ferrando, R. *Phys. Rev. Lett.* **2003**, *90*, 135504.
(13) Rossi, G.; Rapallo, A.; Mottet, C.; Fortunelli, A.; Baletto, F.; Ferrando, R. *Phys. Rev. Lett.* **2004**, *93*, 105503.
(14) Cheng, D.; Huang, S.; Wang, W. *Phys. Rev. B* **2006**, *74*, 064117.
(15) Koutsopoulos, S.; Eriksen, K. M.; Fehrman, R. *J. Catal.* **2006**, *238*, 270.
(16) Devarajan, S.; Bera, P.; Sampath, S. *J. Colloid Interface Sci.* **2005**, *290*, 117.
(17) Barth, J. V.; Costantini, G.; Kern, K. *Nature* **2005**, *437*, 671.
(18) Rao, C. N. R.; Kulkarni, G. U.; Thomas, P. J. *Chem. Soc. Rev.* **2000**, *29*, 27.
(19) Jellinek, J.; Krissinel, E. B. *Chem. Phys. Lett.* **1996**, *258*, 283.
(20) Lloyd, L. D.; Johnston, R. L.; Salhi, S.; Wilson, N. T. *J. Mater. Chem.* **2004**, *14*, 1691.
(21) Montejano-Carrizales, J. M.; Iniguez, M. P.; Alonso, J. A. *Phys. Rev. B* **1994**, *49*, 16649.
(22) Rey, C.; Garca-Rodeja, J.; Galleg, L. J. *Phys. Rev. B* **1996**, *54*, 2942.
(23) López, M. J.; Marcos, P. A.; Alonso, J. A. *J. Chem. Phys.* **1996**, *104*, 1056.
(24) Hsu, P. J.; Lai, S. K. *J. Chem. Phys.* **2006**, *124*, 044711.
(25) Cheng, D.; Huang, S.; Wang, W. *Eur. Phys. J. D* **2006**, *39*, 41.
(26) Bailey, M. S.; Wilson, N. T.; Roberts, C.; Johnston, R. L. *Eur. Phys. J. D* **2003**, *25*, 41.
(27) Christensen, A.; Stolze, P.; Nørskov, J. K. *J. Phys.: Condens. Matter* **1995**, *7*, 1047.
(28) Shimizu, Y.; Ikeda, K. S.; Sawada, S. *Phys. Rev. B* **2001**, *64*, 075412.
(29) Huang, S.-P.; Balbuena, P. B. *J. Phys. Chem. B* **2002**, *106*, 7225.
(30) Chui, Y. H.; Chan, K.-Y. *Chem. Phys. Lett.* **2005**, *408*, 49.
(31) Liu, H. B.; Pal, U.; Perez, R.; Ascencio, J. A. *J. Phys. Chem. B* **2006**, *110*, 5191.
(32) Rubinovich, L.; Haftel, M. I.; Bernstein, N.; Polak, M. *Phys. Rev. B* **2006**, *74*, 035405.
(33) Sakurai, T.; Hashizume, T.; Jimbo, A.; Sakai, A.; Hyodo, S. *Phys. Rev. Lett.* **1985**, *55*, 514.
(34) Shimizu, H.; Ono, M.; Nakayama, K. *Surf. Sci.* **1973**, *36*, 817.
(35) Rehn, L. E.; Hoff, H. A.; Lam, N. Q. *Phys. Rev. Lett.* **1986**, *57*, 780.
(36) Massalski, T. B. *Binary Alloy Phase Diagrams*; ASM International: Metals Park, OH, 1990.
(37) Mainardi, D. S.; Balbuena, P. B. *Langmuir* **2001**, *17*, 2047.
(38) Mainardi, D. S.; Balbuena, P. B. *Int. J. Quantum Chem.* **2001**, *85*, 580.
(39) Derosa, P. A.; Seminario, J. M.; Balbuena, P. B. *J. Phys. Chem. A* **2001**, *105*, 7917.
(40) Grigoryan, V. G.; Springborg, M. *Phys. Rev. B* **2004**, *70*, 205415.
(41) Grigoryan, V. G.; Alamanova, D.; Springborg, M. *Phys. Rev. B* **2006**, *73*, 115415.
(42) Daw, M. S.; Baskes, M. I. *Phys. Rev. Lett.* **1983**, *50*, 1285.
(43) Daw, M. S.; Baskes, M. I. *Phys. Rev. B* **1984**, *29*, 6443.
(44) Foiles, S. M.; Baskes, M. I.; Daw, M. S. *Phys. Rev. B* **1986**, *33*, 7983.
(45) Internet address: 146.246.250.1.
(46) Daw, M. S.; Foiles, S. M.; Baskes, M. I. *Mater. Sci. Rep.* **1993**, *9*, 251.
(47) Grigoryan, V. G.; Springborg, M. *Chem. Phys. Lett.* **2003**, *375*, 219.
(48) Grigoryan, V. G.; Alamanova, D.; Springborg, M. *Eur. Phys. J. D* **2005**, *34*, 187.
(49) Alamanova, D.; Grigoryan, V. G.; Springborg, M. *Z. Phys. Chem.* **2006**, *220*, 811.
(50) Holland, J. *Adaptation in Natural and Artificial Systems*; University of Michigan Press: Ann Arbor, MI, 1975.
(51) Goldberg, D. E. *Genetic Algorithms in Search, Optimization and Machine Learning*; Addison-Wesley: Reading, MA, 1989.
(52) Dong, Y.; Springborg, M.; Burkhart, M.; Veith, M. *Adv. Comput. Methods Sci. Eng.* **2005**, *4A*, 1010.
(53) Dong, Y.; Burkhart, M.; Veith, M.; Springborg, M. *J. Phys. Chem. B* **2005**, *109*, 22820.
(54) Dong, Y.; Springborg, M., submitted.
(55) Tevekeliyska, V.; Dong, Y.; Springborg, M.; Grigoryan, V. G. *Eur. Phys. J. D* **2007**, *43*, 19.
(56) Kittel, C. *Introduction to Solid State Physics*, 8th ed.; Wiley: New York, 2005.
(57) Zhu, L.; De Pristo, A. E. *J. Catal.* **1997**, *167*, 400.
(58) Hultgren, R.; Desai, P. D.; Hawkins, D. T.; Gleiser, M.; Kelley, K. K. *Selected Values of the Thermodynamic Properties of Binary Alloys*; American Society for Metals: Metals Park, OH, 1973.
(59) Wilson, N. T.; Johnston, R. L. *J. Mater. Chem.* **2002**, *12*, 2913.
(60) Foiles, S. M. *Phys. Rev. B* **1985**, *32*, 7685.
(61) Pasturel, A.; Drchal, V.; Kudrnovsky, J.; Weinberger, P. *Phys. Rev. B* **1993**, *48*, 2704.

JP801837D